Hindawi
Advances in Materials Science and Engineering
Volume 2021, Article ID 5540344, 13 pages
https://doi.org/10.1155/2021/5540344

Research Article

Synthesis of MIL-53(Fe) Metal-Organic Framework Material and Its Application as a Catalyst for Fenton-Type Oxidation of Organic Pollutants

Pham Dinh Du and Pham Ngoc Hoai

Thu Dau Mot University, Thu Dau Mot 75000, Vietnam

Correspondence should be addressed to Pham Dinh Du; dupd@tdmu.edu.vn

Received 17 January 2021; Revised 30 January 2021; Accepted 3 February 2021; Published 11 February 2021

Academic Editor: Ştefan Ţălu

The iron (III) benzene dicarboxylate metal-organic framework material (MIL-53(Fe)) was synthesized with either the solvent-thermal or hydrothermal method under different conditions. The influence of the type of solvents, molar ratio of precursors and solvent, temperature, and reaction time on the structure of MIL-53(Fe) was investigated. The material was characterized by using X-ray diffraction (XRD), Fourier-transform infrared spectroscopy (FT-IR), scanning electron microscopy (SEM), high-resolution transmission electron microscopy (HR-TEM), X-ray photoelectron spectroscopy (XPS), and N_2 adsorption/desorption isotherm. The MIL-53(Fe) structure formed in N′, N-dimethylformamide (DMF) and methanol (MeOH) but not in water. In DMF, the molar ratio of precursors and solvent, temperature, and reaction time had a significant effect on the crystal structure of MIL-53(Fe). Under optimal conditions, MIL-53(Fe) has high crystallinity and a large specific surface area ($S_{BET} = 88.2\ m^2/g$). The obtained MIL-53(Fe) could serve as a potential heterogeneous catalyst to oxidize phenol (PhN), rhodamine B (RhB), and methylene blue (MtB) in the Fenton-like reaction system at the different solution pHs.

1. Introduction

Metal-organic frameworks (MOFs) are porous nanomaterials with large specific surface area and considerable pore volume [1–11]. These materials have attracted a lot of attention from scientists due to their perfect structure and applicability in such fields as gas separation and storage [12–17], molecular sensors [18, 19], adsorption [1–4, 20–22], and catalysis [5–8, 23–27]. MOFs are usually synthesized with the hydrothermal method [5, 22, 28] or the solvent-thermal method [1–3, 5, 6, 8–10, 17, 19, 24, 25, 28]. So far, research on MOFs has mainly focused on discovering new types of MOFs and their applicability in different fields. In the literature, little attention is paid to the detailed examination of the role of synthetic conditions.

Among MOFs, MIL-53 (M^{III}) (MIL: Materials of Institute Lavoisier; M^{III} = Fe, Al, Cr, Sc, Ga, In, ...) with the formula $M^{III}(OH)\cdot(O_2C–C_6H_4–CO_2)\cdot H_2O$ has great chemical flexibility and high chemical stability [3, 28, 29]. Iron (III) benzene dicarboxylate, denoted MIL-53(Fe), is a porous solid. It possesses a three-dimensional structure built from infinite one-dimensional bonds –Fe–O–O–Fe–O–Fe– with 1, 4-benzene dicarboxylate bridges [5, 24]. MIL-53(Fe) opens its pores only in the presence of guest molecules. Unlike other MOF materials, MIL-53(Fe) does not possess a high specific surface area [9]. While Pu et al. [25] claim a large specific surface area of $89.7\ m^2/g$ for MIL-53(Fe), others prove that MIL-53(Fe) has a really small specific surface area [1–3, 6, 30]. The cause of this controversy is probably because these authors have not found the required appropriate synthetic conditions to prepare MIL-53(Fe).

Hydrogen peroxide (H_2O_2) decomposition in the presence of iron catalysts to hydroxyl radicals ($HO^\bullet$) has been widely developed into advanced oxidation processes (AOPs) for application in the environmental treatment. The hydroxyl radical has a strong standard oxidation potential

($E^0(HO^\bullet/H_2O = +2.8\ V_{NHE}$)) and a high bimolecular reaction rate constant (10^8–$10^{11}\ M^{-1}\cdot s^{-1}$). This radical is capable of nonselective oxidation of numerous organic substances to nontoxic products, such as CO_2, H_2O, and inorganic salts. Various types of catalytic iron, including metal salts (in the form of Fe^{2+} or Fe^{3+}), metal oxides (e.g., Fe_2O_3 and Fe_3O_4), and zero-valence metal (Fe^0), have been used in chemical (classical Fenton), photochemical (photo-Fenton), and electrochemical (electro-Fenton) degradation pathways. However, the prevention of iron precipitation remains the bottleneck for iron-based AOPs [31]. This motivates the development of heterogeneous Fenton-like processes. Various researchers have utilized different inorganic and organic materials as a supporting matrix for active iron ions in the heterogeneous Fenton-like process, such as SBA-15 [32], carbon [33], kaolin [34], and MCM-41 [35]. Recently, MIL-53(Fe) has attracted the attention of researchers due to its framework containing iron that acts as the structural nodes functioning as a new photocatalyst [5, 24] and a catalyst in the Fenton-like reaction system [6–8, 25].

MIL-53(Fe) has been successfully synthesized and applied to degrade methyl orange in an ultraviolet-assisted heterogeneous Fenton-like process [36]. In this paper, The detailed synthetic conditions will be presented. The influence of solvent type, solvent content, temperature and time of reaction, and the molar ratio of precursors has been investigated to produce MIL-53(Fe) with high crystallinity and a large specific surface area. Addition, the obtained material is used as a catalyst in the Fenton-like reaction system to oxidize phenol (PhN), rhodamine B (RhB), and methylene blue (MtB).

2. Experimental

2.1. Reagents and Chemicals. Iron chloride hexahydrate ($FeCl_3{\cdot}6H_2O$, 99.1%, Merck, EMD Millipore Corporation, Germany), benzene-1, 4-dicarboxylic acid ($C_8H_6O_4$, 99%, Acros, Janssen Pharmaceuticalaan, Belgium) (denoted BDC), N′, N-dimethylformamide (C_3H_7NO, ≥99.5%, Fisher, Leicestershire, England) (denoted DMF), methanol (CH_3OH, 99.9%, Fisher, Seoul, Korea) (denoted MeOH), phenol (C_6H_5OH, Merck, Germany) (denoted PhN), rhodamine B ($C_{28}H_{31}ClN_2O_3$, HiMedia, India) (denoted RhB), and methylene blue ($C_{16}H_{18}ClN_3S$, Merck, Germany) (denoted MtB) were used in this study.

2.2. Synthesis of Iron (III) Benzene Dicarboxylate. The synthesis of iron (III) benzene dicarboxylate was adapted, Du et al. [5]. In a typical process, a mixture of 1.2469 g $FeCl_3{\cdot}6H_2O$, 0.7663 g BDC, and a quantity of the solvent (or DMF/MeOH/water), such that the molar ratio of the precursors and solvent is 1 : 1 : 400, was placed in a Teflon-lined steel autoclave (volume 200 mL) in an oven at 150°C for 15 hours. A yellow powder was obtained by filtering and drying overnight at 150°C. Then, the powder was cooled to ambient temperature and washed with distilled water, filtered, and dried to obtain iron (III) benzene dicarboxylate.

In addition to the effects of solvent type on the formation of MIL-53(Fe) crystalline phase, the influence of the DMF content, reaction temperature, reaction time, and molar ratio of Fe (III)/BDC was also investigated.

2.3. Characterization. X-ray diffraction (XRD) patterns were recorded on a VNU-D8 Advance Instrument (Bruker, Germany) under Cu $K\alpha$ radiation ($\lambda = 1.5406$ Å). Scanning electron microscopy (SEM) images were obtained on an SEM JMS-5300LV (Japan), and high-resolution transmission electron microscopy (HR-TEM) images were obtained by using a JEM-2100. Fourier-transform infrared spectra (FT-IR) were recorded with a Jasco FT/IR-4600 spectrometer (Japan) in the range of 4000–400 cm^{-1}. The X-ray photoelectron spectroscopy (XPS) was studied by using a Shimadzu Kratos AXIS Ultra DLD spectrometer (Japan). Peak fitting was performed on CasaXPS software. The N_2 adsorption/desorption isotherm measurement test was performed at 77 K on a Tristar 3000 analyzer. Before setting the dry mass, the samples were degassed at 250°C with N_2 for 5 h.

2.4. Determination of the Point of Zero Charge. The point of zero charge (pH_{PZC}) of the MIL-53(Fe) material was determined following the process described by Jing et al. [23]. 50 mL of NaCl 0.01 M solution was added to a series of 100 mL Erlenmeyer flasks. The initial pH value of the solutions (pH_i) was adjusted to 2–12 by adding either the HCl 0.1 M or NaOH 0.1 M solution. Then, 0.05 g of MIL-53(Fe) was added to each flask, and the mixture was shaken for 48 hours. The final pH (pH_f) of the solutions was measured. The plot representing the relationship between the difference of the final and initial pH value ($\Delta pH = pH_f - pH_i$) and pH_i was drawn, and the point of intersection of the curve with the abscissa provides pH_{PZC}.

2.5. Oxidizing Organic Compounds. The oxidation of PhN, RhB, and MtB by H_2O_2 in the aqueous solution was carried out at 30°C in a 500 mL round flask with a reflux condenser in the presence of MIL-53(Fe). In each experiment, 0.05 g of the catalyst was stirred for 30 minutes with 100 mL of a solution containing PhN (or RhB, or MtB) at a specific concentration and pH (the pH of the solution was adjusted with a solution of HCl 0.1 M or NaOH 0.1 M) to achieve adsorption/desorption equilibrium. Then, H_2O_2 was added to the solution (the concentration of H_2O_2 in the solution is 0.096 M). After a certain interval, 5 mL of the solution was withdrawn and centrifuged to remove the catalyst, and the concentration of the remaining solution was determined. The experiments were carried out in three replicates, and the data were analyzed using Microsoft Excel software.

The concentration of PhN in the solution was determined with high-performance liquid chromatography (HPLC) on the UFLC Shimadzu (Japan) equipment. The HPLC apparatus was equipped with a C-18 column with an acetonitrile/methanol/water (1 : 1 : 8) mobile phase and an SPD-20A detector at a wavelength of 254 nm. The products

of PhN oxidation were determined with the LC-MS/MS method on the Agilent 1900/6500 series Q-TOF (USA).

The RhB (or MtB) concentration in the supernatant was determined with the UV-Vis method on the Jasco V-770 (Japan) at $\lambda_{max} = 554$ nm for RhB ($\lambda_{max} = 664$ nm for MtB).

3. Results and Discussion

3.1. Structural Properties of Iron (III) Benzene Dicarboxylate Synthesized under Different Conditions

3.1.1. Influence of Solvent Type. The influence of DMF, MeOH, and water on the formation of the crystal structure of iron (III) benzene dicarboxylate is evaluated from XRD data. The XRD patterns of the samples synthesized in DMF and MeOH exhibit diffraction peaks at 7.24, 8.92, 9.72, 10.15, and 12.50° (Figure 1(a)). These peaks indicate that the metal-organic framework structure is formed in the reaction. However, the sample synthesized in MeOH has diffraction peaks with higher 2θ at 17, 25, and 27.6° (Figure 1(b)), and they are the typical diffraction peaks for BDC. This evidence indicates that a large amount of BDC does not react or only binds with iron (III) in the form of individual structures (not forming a framework). The sample synthesized in water also exhibits only the characteristic diffraction peaks of BDC without diffraction peaks at smaller angles (Figure 1(b)). This finding indicates that water is not a suitable solvent for the formation of the MIL-53(Fe) structure.

The MIL-53(Fe) structure is formed via the bonds between iron (III)/iron oxide and the BDC anion, and therefore, the number of these bonds has a significant influence on the synthesis efficiency. When the solvent is MeOH and water, iron (III) easily hydrolyzes at high temperatures. In contrast, DMF is suitable for the deprotonation of BDC to form BDC anions because the dipole moment of DMF is much greater than that of MeOH and water (3.86 as opposed to 1.69 and 1.85 D). Among the three solvents, DMF is the most suitable for the synthesis of MIL-53(Fe). Numerous authors report their synthesis of MIL-53(Fe) in DMF [1–3, 5, 6, 8–10, 19, 24, 25, 28].

The FT-IR spectra of BDC and the iron (III) benzene dicarboxylate samples synthesized in the solvents are shown in Figure 2. For BDC, the absorption peak at 1681 cm^{-1} characterizes the stretching vibration of the C = O group, and the absorption peaks at 1423 and 937 cm^{-1} are attributed to the bending vibration of the O–H group, while the absorption peak at 784 cm^{-1} represents the stretching vibration of the C–H bond in the aromatic ring [24]. For the sample synthesized in water, the absorption peaks are almost identical to those of BDC, indicating that the MIL-53(Fe) structure is hardly formed. The absorption peak of ν_{Fe-O} at 565 cm^{-1} is probably due to the iron hydroxide formed by hydrolysis. For the sample synthesized in MeOH, the appearance of the absorption peak at 1508 cm^{-1} indicates the existence of a coordinated bond between the central metal atom and the carboxyl groups, and the absorption peak at 559 cm^{-1} corresponds to the stretching vibration of Fe–O. These absorption bands indicate the formation of the metal-oxo bonds between the carboxylic group of BDC acids and Fe (III) [1, 6, 24]. These bonds indicate the presence of the MIL-53(Fe) metal-organic framework. However, the absorption peak characteristic for the stretching vibration of the C = O group (1704 cm^{-1}) remains intense, manifesting that a large amount of BDC is not involved in the formation of the framework. For the sample synthesized in DMF, the absorption peaks at 1529, 1383, 748, and 537 cm^{-1} characterize the structure of the MIL-53(Fe) material [1, 6, 24]. Furthermore, the absorption band at 1681 cm^{-1} ($\nu_{C=O}$) almost disappears, indicating that the obtained MIL-53(Fe) sample no longer has free carboxylic groups, and they form bonds with Fe (III). These results are completely consistent with the XRD results presented in Figure 1.

The SEM images indicate that the material synthesized in DMF consists of rods of varying sizes with a smooth surface, sharp edge, and multiple cracks/fractures (Figures 3(a) and 3(b)). The cracks/fractures in the material structure are probably responsible for the MIL-53(Fe) characteristic diffraction with low intensity, as seen in Figure 1(a). In MeOH, the obtained sample also has a rod form (Figure 3(c)) similar to the sample synthesized in DMF, but the rod shape is irregular, and the surface has small particles attached to it. For the sample synthesized in water (Figure 3(d)), the obtained material has a cube shape with a size of 1–2 μm and a relatively regular nodule surface.

Thus, DMF and MeOH enable the formation of the MIL-53(Fe) structure with similar morphology. The metal-organic framework structure is not formed in water. Therefore, the cubes are probably encapsulated compounds with iron oxide clusters in the core, and the surface consists of various forms of benzene dicarboxylate bridges.

3.1.2. Influence of Solvent Content and Reaction Temperature. In this section, DMF is used as a solvent to synthesize iron (III) benzene dicarboxylate. At a low solvent content ratio (the molar ratio of precursors and DMF is 1 : 1 : 200), low intensity of diffraction peaks indicates low crystallinity of the material (Figure 4(a)). At the 1 : 1 : 300 ratio, the obtained material exhibits a high-intensity diffraction peak at 12.5°, indicating the metal-organic framework formation, but the remaining diffraction peaks have low intensity, indicating a low-ordered material. At higher solvent content ratios (1 : 1 : 400 and 1 : 1 : 450), the XRD patterns have diffraction peaks at 9.29, 12.23, 17.68, 24.82, and 26.92° with higher intensity and clarity, manifesting that the metal-organic framework structure is formed with high crystallinity.

When synthesized at 120°C, MIL-53(Fe) exhibits a low crystal structure with low intensity on the XRD pattern (Figure 4(b)). The peak intensity increases when the synthesis is performed at 150°C, and the material is crystalline. This crystalline structure practically disappears at higher synthetic temperatures (180 and 200°C). Thus, at the molar ratio of the precursors and DMF of 1 : 1 : 450 and 150°C, MIL-53(Fe) possesses a highly crystalline structure.

The SEM image and FT-IR spectrum of the iron (III) benzene dicarboxylate sample synthesized at 150°C and a precursors/DMF molar ratio of 1 : 1 : 450 are shown in Figure 5. The obtained sample has a full band of absorption

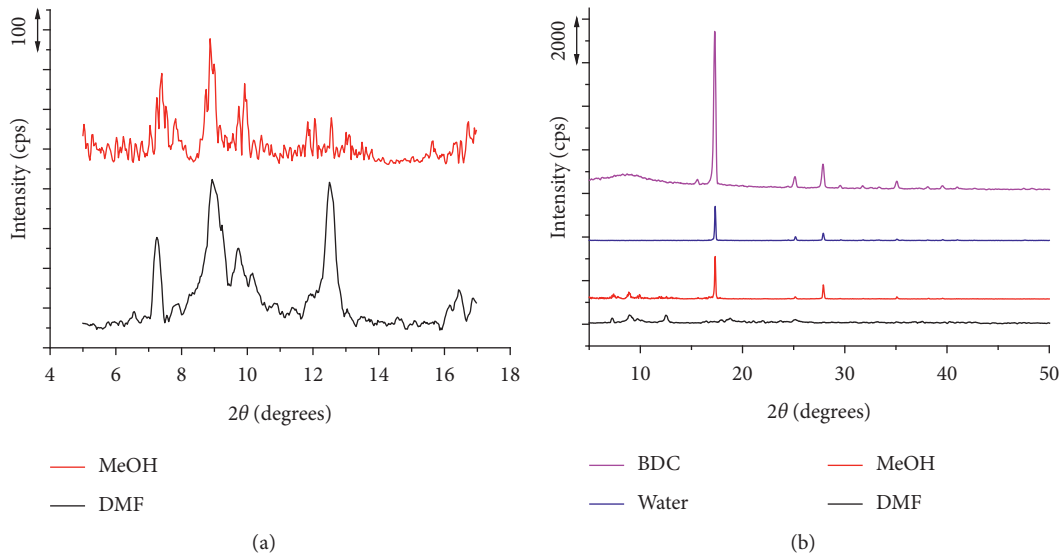

Figure 1: XRD patterns of iron (III) benzene dicarboxylate samples: (a) synthesis in MeOH and DMF (small angle); (b) synthesis in different solvents (the BDC sample for comparison).

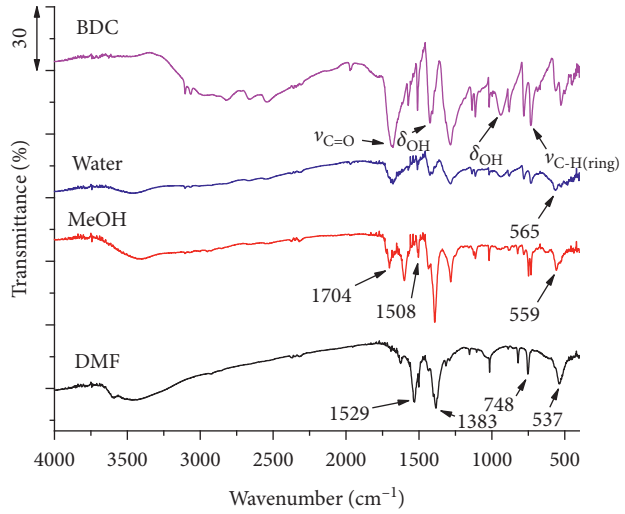

Figure 2: FT-IR spectra of iron (III) benzene dicarboxylate samples synthesized in the solvents and BCD.

characteristics for MIL-53(Fe) with strong intensities at 1526, 1380, 751, and 535 cm^{-1} [1, 6, 24]. No vibration for $\nu_{C=O}$ is observed, indicating that all BDC is consumed in the reaction. The morphology of the obtained material is similar to that of the sample synthesized at the 1 : 1 : 400 ratio (Figure 3(a)) with a more regular shape and smoother surface.

3.1.3. Influence of Reaction Time and Molar Ratio Fe (III)/BDC. To investigate the influence of reaction time on the formation of the metal-organic framework structure, the reaction temperature (150°C) and the molar ratio of Fe (III)/BCD/DMF (1 : 1 : 450) are fixed. The X-ray diffraction patterns of the iron (III) benzene dicarboxylate samples show that the peaks at $2\theta < 30°$ and characteristic for metal-organic framework materials have low intensity and decrease with increasing reaction time (Figure 6(a)). Meanwhile, the peaks at 24.09, 33.19, 35.71, 41.05, 49.59, and 54.04° corresponding to the (012), (104), (110), (113), (024), and (116) planes of iron oxide (α-Fe_2O_3) [37] have high intensity. This increasing intensity proves that when the reaction time is extended, the MIL-53(Fe) structure is broken, and under these conditions, mainly iron oxide clusters are formed.

However, for the samples synthesized at the molar ratios of Fe (III)/BDC at 1 : 2 or 1 : 3, the XRD patterns have diffraction peaks at 9.17, 12.59, 17.51, 18.17, 18.47, and 25.37° (Figure 6(b)), which are consistent with those reported in various publications on the MIL-53(Fe) material [1, 5, 6, 8, 19, 24, 25]. And the diffraction peaks of iron oxide do not appear. Therefore, the MIL-53(Fe) metal-organic framework material is formed with high purity at the molar ratios of Fe (III)/BDC at 1 : 2 or 1 : 3. In particular, the intensity of the peaks characteristic for the MIL-53(Fe) material is high and sharp when synthesized at the molar ratio of Fe (III)/BDC at 1 : 2, demonstrating that the MIL-53(Fe) structure is formed with high order and crystallinity.

The infrared spectra of the iron (III) benzene dicarboxylate samples synthesized at 150°C with different reaction times and different molar ratios of Fe (III)/BDC are depicted in Figure 7. The samples are synthesized at the ratio of 1 : 1 and 1 : 2 and 24 h have absorption bands at 1528, 1383, 750, and 542 cm^{-1}. These bands are specific to MIL-53(Fe) [1,6,24], indicating the formation of a metal-organic framework structure. However, the sample synthesized at the ratio 1 : 1 still has free BDC, evidenced by the vibration band of ν (C = O) at 1693 cm^{-1}. For the sample synthesized at the ratio 1 : 1 and 96 h, the intensity of the specific absorption bands of MIL-53(Fe) significantly reduces. Therefore, longer reaction time does not support the formation of the metal-organic framework, and under this condition, mainly iron oxide is formed.

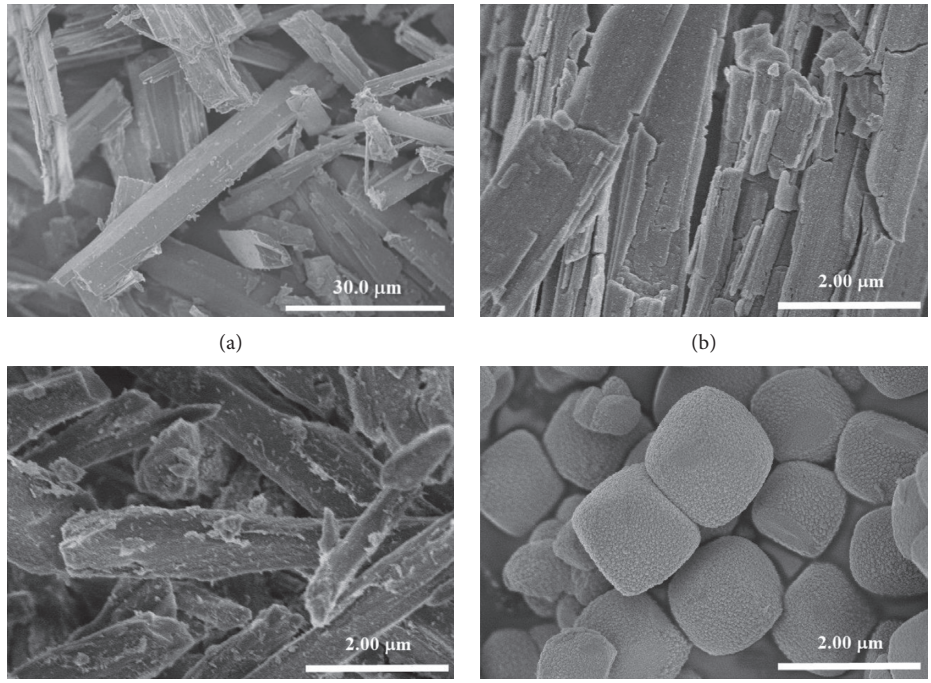

Figure 3: SEM images of iron (III) benzene dicarboxylate samples synthesized in DMF (a), (b), MeOH (c), and water (d).

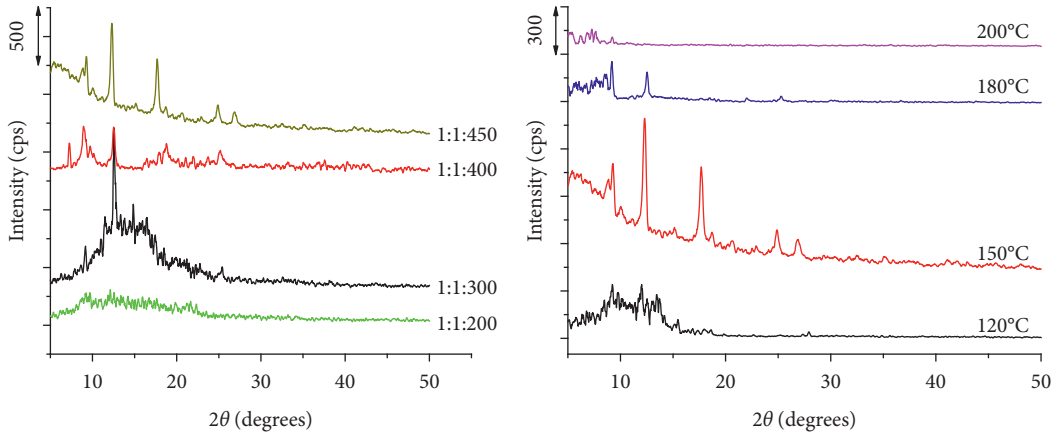

Figure 4: XRD patterns of iron (III) benzene dicarboxylate samples: (a) synthesized at 150°C and different solvent contents; (b) synthesized at different temperatures with a precursors/DMF molar ratio of 1 : 1 : 450.

The morphology of the iron (III) benzene dicarboxylate samples synthesized at 150°C with different reaction times and different molar ratios of Fe (III)/BDC indicates that at the ratio of 1 : 2 and 24 h (Figure 8(a)), the material has a shape of rods with a smooth surface and sharp edges (similar to those observed in Figures 3(a) and 5(b)). At high resolution, little cracking/fracture is observed inside the rods (Figure 8(b)). At the ratio of 1 : 1 and 24 h (Figure 8(c)), the material has a spherical shape with a particle diameter of about 0.3–0.4 μm, with interspersed larger plate particles. When the reaction time is extended to 96 h, the particles are mainly spherical (Figure 8(d)).

The HR-TEM images of the iron (III) benzene dicarboxylate samples synthesized at 150°C and 24 h show an interplanar spacing distance of about 0.25 nm, corresponding to the (110) plane of α-Fe_2O_3 [37] on the sample synthesized with the ratio of Fe (III)/BDC at 1 : 1 (Figures 9(a) and 9(b)). This finding is consistent with the XRD result presented in Figure 6(a), indicating the formation of iron oxide clusters in the material. In Figure 9(b), it is also possible to see worm-hole-like structures illustrating the appearance of the MIL-53(Fe) metal-organic framework. At the ratio of Fe (III)/BDC 1 : 2 and 24 h, the material has honeycomb-like structures with a diameter of

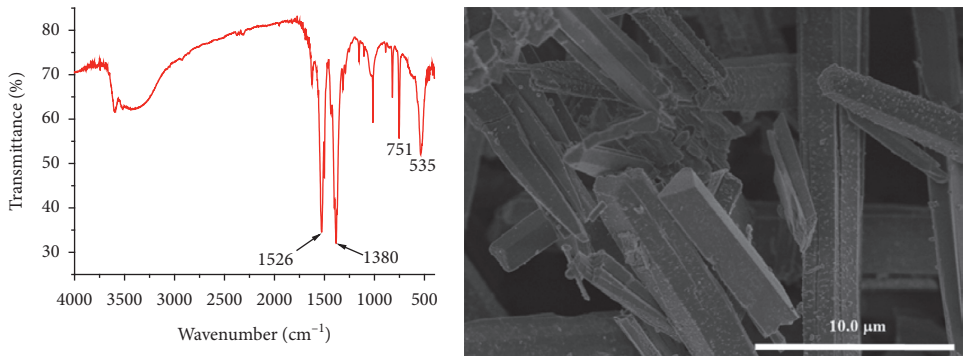

Figure 5: FT-IR spectra (a) and SEM image (b) of the iron (III) benzene dicarboxylate sample synthesized at 150°C and precursors/DMF molar ratio of 1 : 1 : 450.

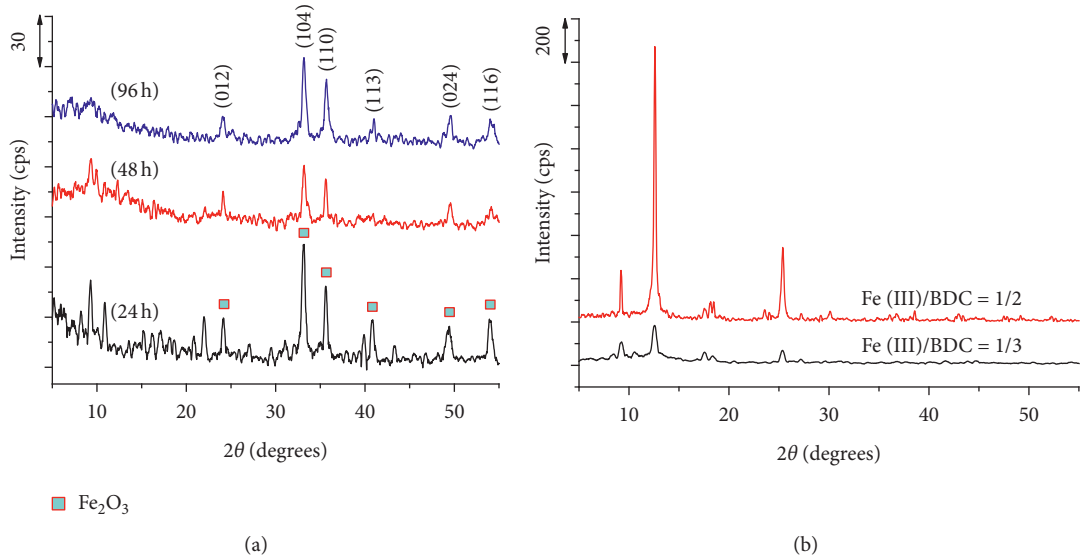

Figure 6: XRD patterns of iron (III) benzene dicarboxylate samples synthesized at 150°C: (a) different reaction times; (b) different molar ratios of Fe (III)/BDC (reaction time of 24 h.

about 20–30 nm (Figure 9(c)). At higher magnification, the HR-TEM image shows worm-hole-like structures (Figure 9(d)), indicating that the metal-organic framework structure is very uniform with high purity.

The XPS survey spectra of the samples (Figures 10(a) and 10(c)) confirm the presence of Fe, C, and O elements on the surface of the samples. Figures 10(b) and 10(d) show the high-resolution XPS spectra of Fe 2p with two peaks corresponding to the binding energy of 709.3–709.4 eV and 722.1–722.5 eV, which are assigned to Fe $2p_{3/2}$ and Fe $2p_{1/2}$ of Fe (III), respectively [1, 5, 24]. The peak separation, namely, $\Delta Fe2p = 2p_{1/2} - 2p_{3/2} \approx 13$ eV, is very similar to the theoretical value of 13.6 eV for Fe_2O_3 [38]. Therefore, these peaks belong to Fe^{3+} of the iron (III) benzene dicarboxylate samples.

The nitrogen adsorption-desorption isotherms reveal that the iron (III) benzene dicarboxylate samples synthesized under different conditions exhibit between type I and type IV, with microporous and mesoporous structure (Figure 11). The samples undergo condensation at relatively high pressure ($P/P_0 \sim 1$) with a H3-type hysteresis loop, indicating the existence of the pores formed between particles of uneven sizes. For the sample synthesized at the molar ratio of Fe (III)/BDC 1 : 2, strong condensation at low relative pressures indicates the existence of multiple micropores. The textural properties of the samples are presented in Table 1. The specific surface area increases gradually with the crystallinity of the synthesized MIL-53(Fe) material and reaches the highest value (88.2 m^2/g) for the sample synthesized with the molar ratio 1 : 2. This value is consistent with that reported by Pu et al. [25] (77.6–89.7 m^2/g) for MIL-53(Fe) and much higher than the value reported in other publications [1–3, 6, 30] (from 5.5 to 52 m^2/g).

In summary, the optimal conditions for forming the MIL-53(Fe) material in this study are as follows: solvent DMF, molar ratio of Fe(III)/BDC/DMF 1 : 2 : 450,

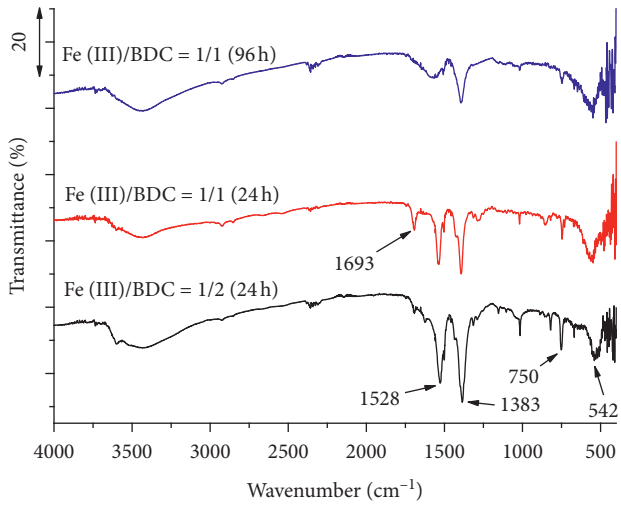

Figure 7: FT-IR spectra of iron (III) benzene dicarboxylate samples synthesized at 150°C with different reaction times and different Fe (III)/BDC molar ratios.

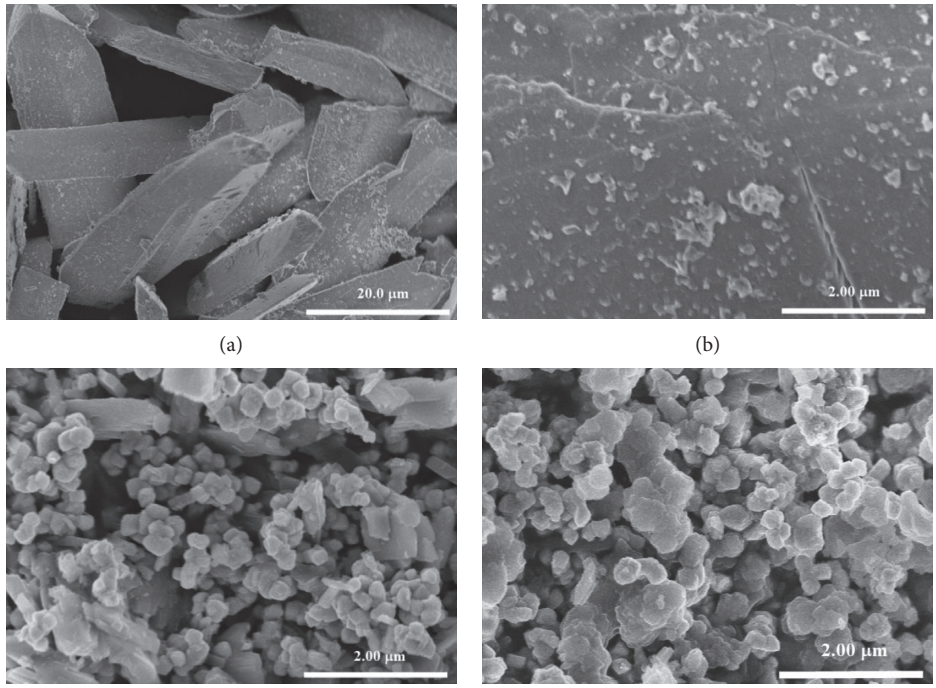

Figure 8: SEM images of iron (III) benzene dicarboxylate samples synthesized at 150°C with different reaction times and different molar ratios of Fe (III)/BDC: (a), (b) 1 : 2, 24 h; (c) 1 : 1, 24 h; and (d) 1 : 1, 96 h.

temperature 150°C, and reaction time 24 h. This MIL-53(Fe) sample is used as the catalyst for the Fenton-like process to oxidize organic substances in aqueous solutions.

3.2. Catalytic Activity of MIL-53(Fe). The homogenous Fenton reaction is strongly restricted by the pH of the solution because Fe^{3+} does not exist at pH ≥ 4 and forms ferric hydroxide sludge. The optimal working pH range for a homogenous Fenton reaction is 2.8–3.2 [31, 39]. Therefore, heterogeneous Fenton-like processes are developed, in which the catalysts containing iron species (mostly Fe^{3+}) are stabilized by confining in substrates, and they create $HO^{\bullet}$ radicals under uncontrolled pH conditions. MIL-53(Fe) is a metal-organic framework material with Fe (III) (or iron clusters) structural nodes, and it can be used as a heterogeneous catalyst in heterogeneous Fenton-like reactions. Therefore, in this section, the catalytic activity of MIL-53(Fe) is assessed via the oxidation of phenol (PhN), rhodamine B (RhB), and methylene blue (MtB) at different solution pHs in a Fenton-like reaction system. The decomposition efficiency of the organic compounds is depicted in Figure 12.

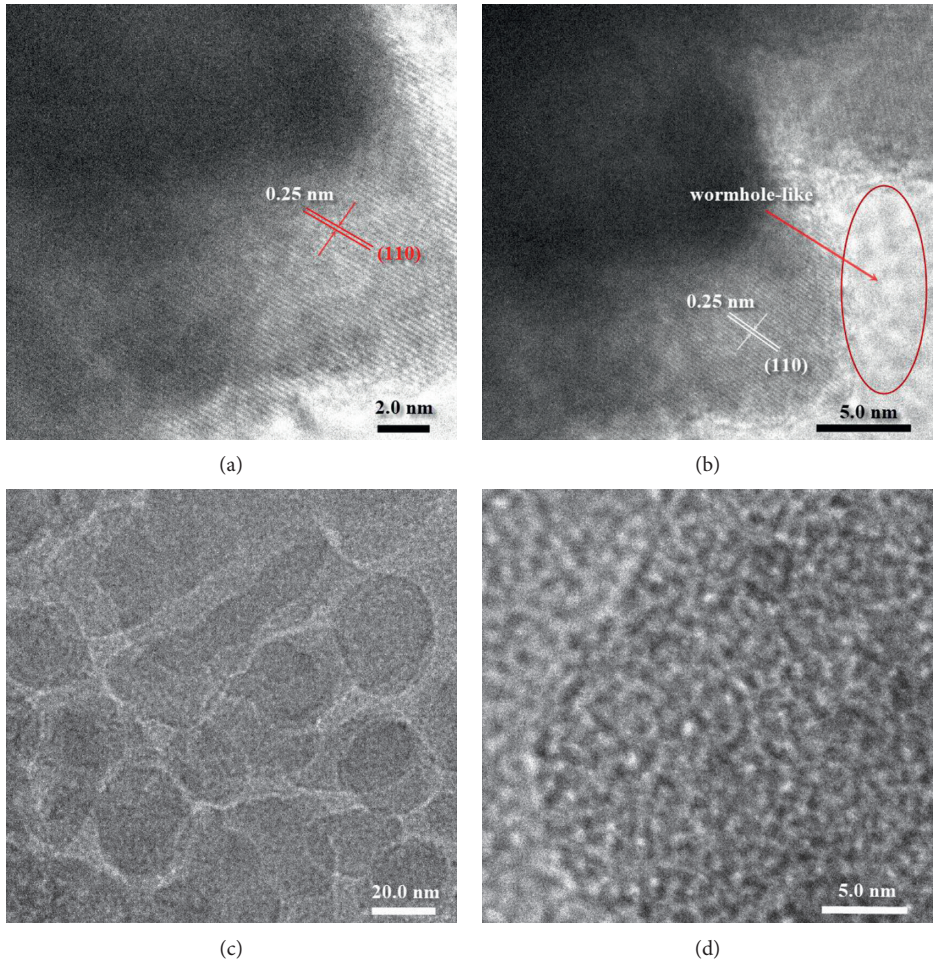

Figure 9: HR-TEM images of iron (III) benzene dicarboxylate samples synthesized at 150°C and 24 h with different Fe (III)/BDC molar ratios: (a), (b) 1 : 1; (c), (d) 1 : 2.

Figure 12(a) shows that the PhN decomposition efficiency is approximately 100% after only 20 minutes of reaction at pH 2–4. In the pH range 6–10, the PhN decomposition rate decreases gradually. After 20 minutes, the efficiency reaches 96% at pH = 6, 90% at pH = 8, and only 52% at pH = 10. It does not reach ~100% until after 40–60 minutes of reaction. Meanwhile, at pH 12, the decomposition efficiency of PhN is very low, only achieving ~23% after 120 minutes of reaction. It is well known that PhN is a very stable compound and difficult to decompose completely by a catalytic oxidation reaction. However, the HPLC data presented in Figure 12(b) show that PhN decomposes almost completely after 40 minutes of reaction in the pH range 2–10, and the remaining intermediate product is mainly formic acid in the pH range 2–8. This indicates that MIL-53(Fe) is applicable to catalyze the complete oxidation of PhN in an aqueous solution by H_2O_2.

The influence of pH on the efficiency of decomposition of RhB by H_2O_2 on MIL-53(Fe) catalyst is depicted in Figure 12(c). At pH = 2, RhB decomposes very quickly. After 30 minutes of reaction, the efficiency is 93%, and it decomposes completely after 60 minutes. In the pH range 4–10, the efficiency remains stable in the first period and reaches approximately 100% after 90 minutes of reaction. At pH = 12, the decomposition of RhB is slow, and the efficiency does not reach 50% until after 120 minutes of reaction.

As for MtB (Figure 12(d)), at pH = 2, this dye decomposes very quickly with a 98% efficiency only after 15 minutes of reaction and 100% after 20 minutes. In the pH range 4–8, the decomposition rate is practically stable, and the dye decomposes completely after 120 minutes of reaction. At pH 10 or 12, MtB also decomposes completely after 120 reactions, but the rate of MtB decomposition at pH 12 is higher. Over half of methylene blue decomposes (56%) after 15 minutes of reaction, compared with 18% at pH 10.

In summary, the MIL-53(Fe) material has catalytic activity over a wide pH range (2–12), indicating that this is a heterogeneous Fenton catalyst, i.e., iron in the material does not dissolve in solution to form a homogenous Fenton system. With all three pollutants, the decomposition rate is high in the pH range of 2–10. At pH 12, the decomposition rate of PhN and RhB decreases, while MtB decomposes faster. It is obvious that the surface of the MIL-53(Fe) material becomes negative at high pH due to the adsorption of OH^- ions from solution (pH_{PZC} of MIL-53(Fe) is 3.3, Figure 13). At this pH, PhN exists as an anion (PhN^-), and

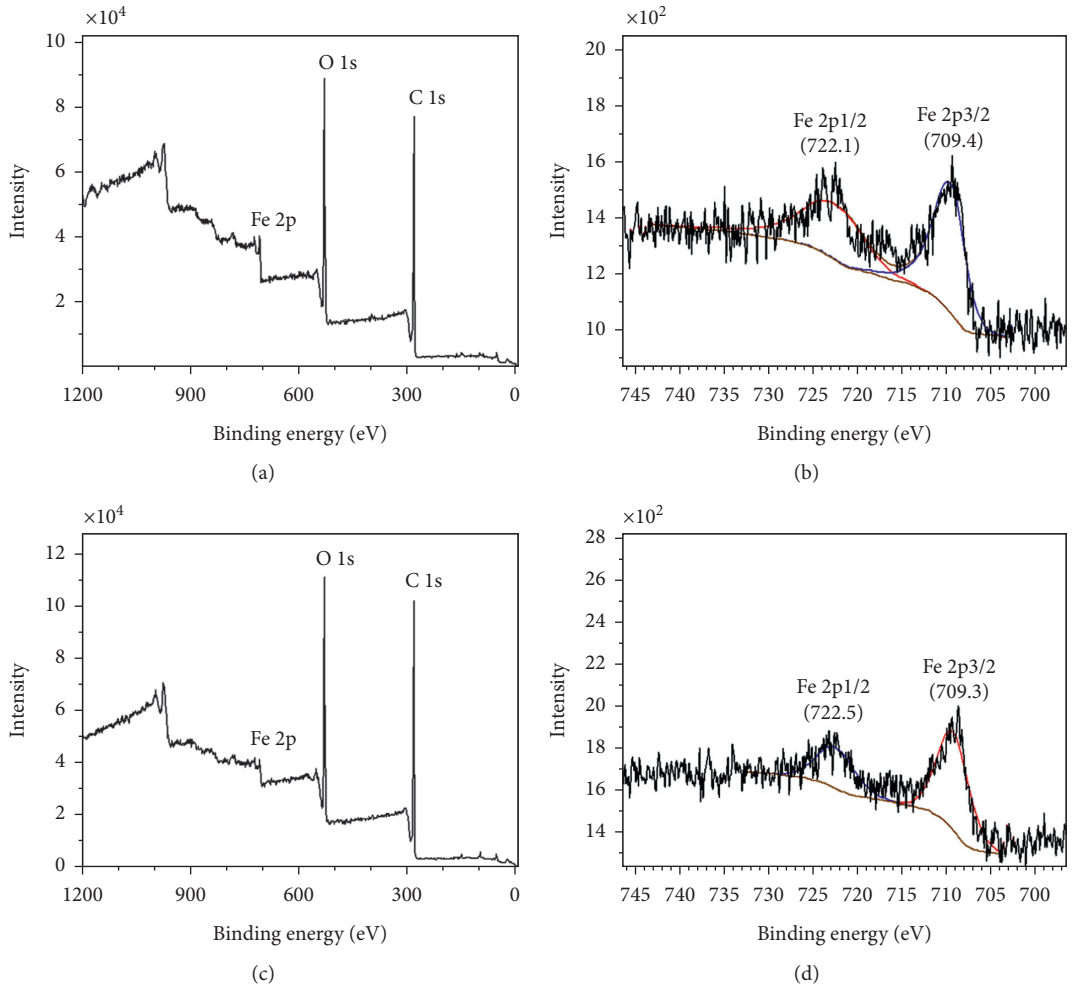

Figure 10: XPS spectra of iron (III) benzene dicarboxylate samples synthesized at 150°C and 24 h with different Fe (III)/BDC molar ratios: (a), (b) 1 : 1; (c), (d) 1 : 2.

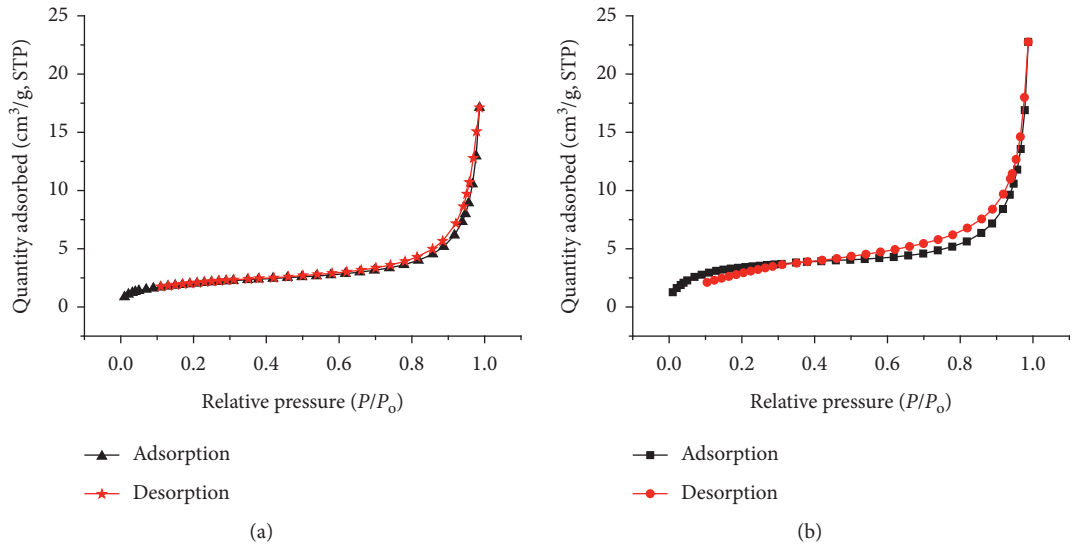

Figure 11: Continued.

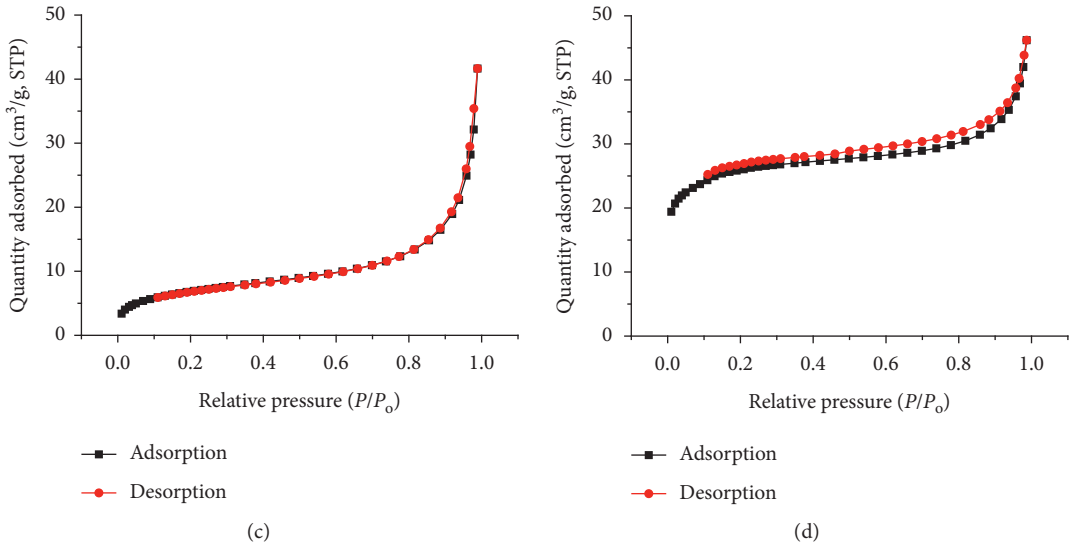

Figure 11: Nitrogen adsorption-desorption isotherms of iron (III) benzene dicarboxylate samples synthesized under different conditions: (a) MeOH, molar ratio of 1 : 1:400, 150°C, and 15 h; (b) DMF, molar ratio 1 : 1:400, 150°C, and 15 h; (c) DMF, molar ratio 1 : 1:450, 150°C, and 15 h; and (d) DMF, molar ratio 1 : 2:450, 150°C, and 24 h.

Table 1: Textural properties of iron (III) benzene dicarboxylate samples synthesized under different conditions.

Solvent	Synthesized conditions		Specific surface area, S_{BET} ($m^2 \cdot g^{-1}$)	Micropore area ($m^2 \cdot g^{-1}$)	External surface area ($m^2 \cdot g^{-1}$)
	Molar ratio of Fe (III)/BDC/solvent	Temperature and time			
MeOH	1 : 1 : 400	150°C for 15 h	7.3	3.6	3.7
DMF	1 : 1 : 400	150°C for 15 h	12.4	8.8	3.6
DMF	1 : 1 : 450	150°C for 15 h	24.6	9.6	15.0
DMF	1 : 2 : 450	150°C for 24 h	88.2	77.0	11.2

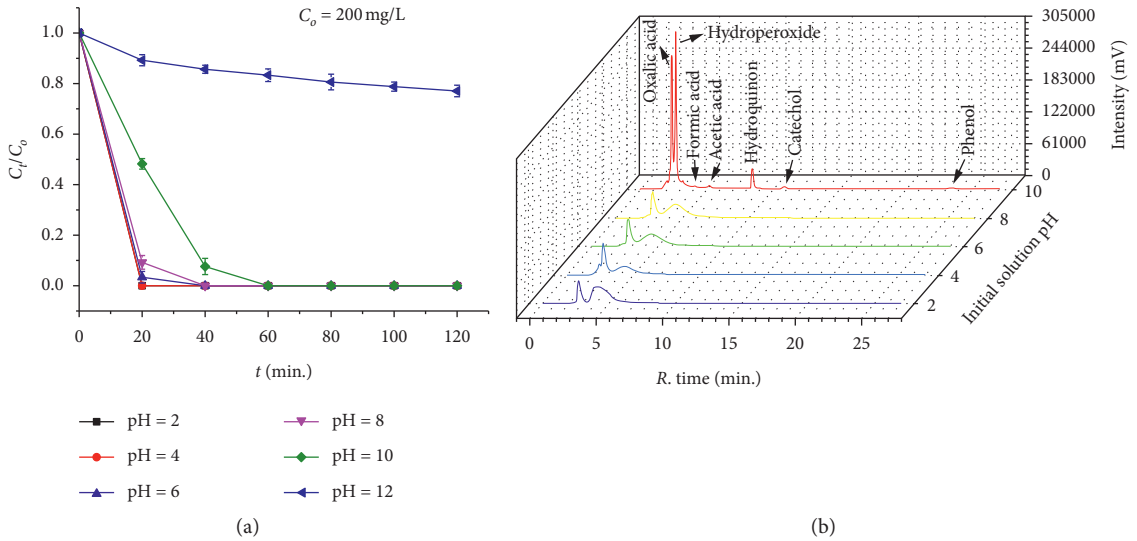

Figure 12: Continued.

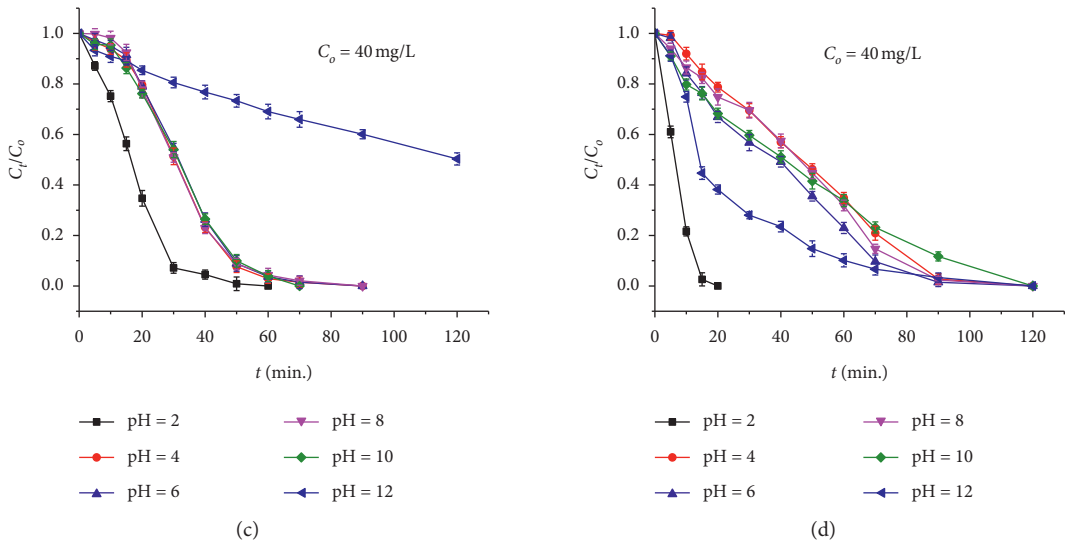

Figure 12: Decomposition of organic compounds by H_2O_2 on MIL-53(Fe) catalyst at different initial solution pHs: (a) PhN; (b) HPLC chromatograms of the PhN oxidation reaction solution after 40 minutes of reaction; (c) RhB; (d) MtB.

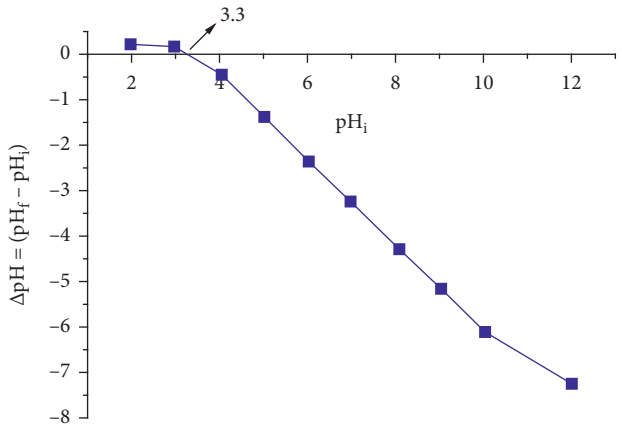

Figure 13: The plot for determination of point of zero charge of MIL-53(Fe).

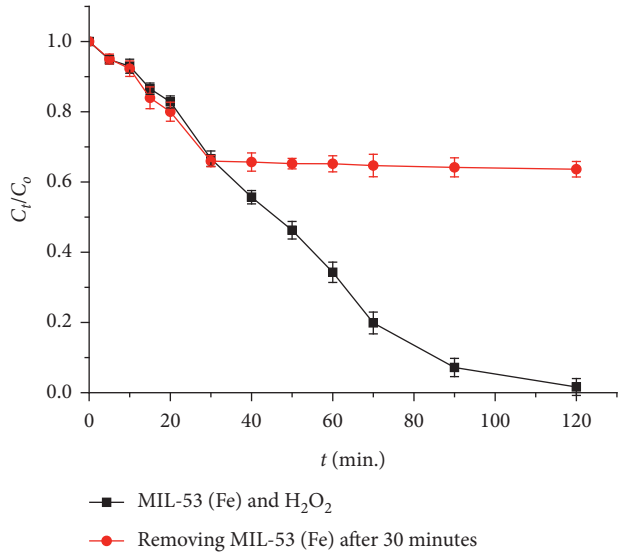

Figure 14: Leaching experiments (experimental conditions: 0.5 g/L of catalyst; 80 mg/L RhB; 0.096 M H_2O_2; 30°C, pH 7).

therefore, the electrostatic repulsion hinders its adsorption, leading to a significant reduction of the decomposition rate. RhB exists in the form of "closed" entirety in the alkaline environment (electrically neutral), so the rate of decomposition also decreases. In contrast, MtB exists as a cation (MtB^+), and it adsorbs onto the surface of MIL-53(Fe) (due to electrostatic interactions), causing the rate of MtB degradation to increase.

To determine whether iron in the catalyst dissolves in the reaction solution, a leaching experiment is also conducted by monitoring the solution after filtering out the MIL-53(Fe) catalyst by centrifugation after 30 minutes of reaction. It is clearly that the degradation of RhB is quenched although H_2O_2 remains in the solution (Figure 14). This finding confirms that MIL-53(Fe) acts as a heterogeneous catalyst in this oxidation process.

4. Conclusions

The present paper shows that the MIL-53(Fe) metal-organic framework material is successfully synthesized with the solvent-thermal method with DMF or MeOH as solvents, where DMF is more suitable. In addition, the molar ratio of precursors and solvents, temperature, and reaction time also significantly influence the formation of MIL-53(Fe). In DMF and the molar ratio Fe (III)/BDC of 1 : 2, the resulting MIL-53(Fe) has high crystallinity, a large specific surface area (S_{BET} 88.2 $m^2 \cdot g^{-1}$), and an even porous structure. MIL-53(Fe) is a potential heterogeneous Fenton catalyst for the

oxidation of organic pollutants in the aqueous environment by hydrogen peroxide over the pH range 2–12.

Data Availability

The data used to support the findings of this study are available from the corresponding author upon request.

Conflicts of Interest

The authors declare that they have no conflicts of interest.

References

[1] T. A. Vu, G. H. Le, C. D. Dao et al., "Arsenic removal from aqueous solutions by adsorption using novel MIL-53 (Fe) as a highly efficient adsorbent," *RSC Advances*, vol. 5, no. 7, pp. 5261–5268, 2015.

[2] E. Yilmaz, E. Sert, and F. S. Atalay, "Synthesis, characterization of a metal organic framework: MIL-53 (Fe) and adsorption mechanisms of methyl red onto MIL-53 (Fe)," *Journal of the Taiwan Institute of Chemical Engineers*, vol. 65, pp. 323–330, 2016.

[3] S. Naeimi and H. Faghihian, "Application of novel metal organic framework, MIL-53 (Fe) and its magnetic hybrid: for removal of pharmaceutical pollutant, doxycycline from aqueous solutions," *Environmental Toxicology and Pharmacology*, vol. 53, pp. 121–132, 2017.

[4] M. H. M. Tahir, S. E. Teo, and P. Y. Moh, "Removal of methylene blue by iron terephthalate metal-organic framework/polyacrylonitrile membrane," *Transactions on Science and Technology*, vol. 4, no. 1, pp. 14–21, 2017.

[5] J.-J. Du, Y.-P. Yuan, J.-X. Sun et al., "New photocatalysts based on MIL-53 metal-organic frameworks for the decolorization of methylene blue dye," *Journal of Hazardous Materials*, vol. 190, no. 1–3, pp. 945–951, 2011.

[6] L. Ai, C. Zhang, L. Li, and J. Jiang, "Iron terephthalate metal-organic framework: revealing the effective activation of hydrogen peroxide for the degradation of organic dye under visible light irradiation," *Applied Catalysis B: Environmental*, vol. 148-149, pp. 191–200, 2014.

[7] X. Liu, Y. Zhou, J. Zhang, L. Tang, L. Luo, and G. Zeng, "Iron containing metal-organic frameworks: structure, synthesis, and applications in environmental remediation," *ACS Applied Materials & Interfaces*, vol. 9, no. 24, pp. 20255–20275, 2017.

[8] M. Pu, Z. Guan, Y. Ma et al., "Synthesis of iron-based metal-organic framework MIL-53 as an efficient catalyst to activate persulfate for the degradation of orange G in aqueous solution," *Applied Catalysis A: General*, vol. 549, pp. 82–92, 2018.

[9] J. Gordon, H. Kazemian, and S. Rohani, "Rapid and efficient crystallization of MIL-53 (Fe) by ultrasound and microwave irradiation," *Microporous and Mesoporous Materials*, vol. 162, pp. 36–43, 2012.

[10] E. Haque, N. A. Khan, J. H. Park, and S. H. Jhung, "Synthesis of a metal-organic framework material, iron terephthalate, by ultrasound, microwave, and conventional electric heating: a kinetic study," *Chemistry-A European Journal*, vol. 16, no. 3, pp. 1046–1052, 2010.

[11] Ş. Ţălu, *Micro and Nanoscale Characterization of Three Dimensional Surfaces. Basics and Applications*, Napoca Star Publishing House, Cluj-Napoca, Romania, 2015.

[12] T. K. Trung, P. Trens, N. Tanchoux et al., "Hydrocarbon adsorption in the flexible metal organic frameworks MIL-53 (Al, Cr)," *Journal of the American Chemical Society*, vol. 130, no. 50, pp. 16926–16932, 2008.

[13] V. Finsy, L. Ma, L. Alaerts, D. E. De Vos, G. V. Baron, and J. F. M. Denayer, "Separation of CO_2/CH_4 mixtures with the MIL-53 (Al) metal-organic framework," *Microporous and Mesoporous Materials*, vol. 120, no. 3, pp. 221–227, 2009.

[14] P. Rallapalli, D. Patil, K. P. Prasanth, R. S. Somani, R. V. Jasra, and H. C. Bajaj, "An alternative activation method for the enhancement of methane storage capacity of nanoporous aluminium terephthalate, MIL-53 (Al)," *Journal of Porous Materials*, vol. 17, no. 5, pp. 523–528, 2010.

[15] W. D. Malsche, S. V. D. Perrer, S. Silverans et al., "Unusual pressure-temperature dependency in the capillary liquid chromatographic separation of C8 alkylaromatics on the MIL-53 (Al) metal-organic framework," *Microporous and Mesoporous Materials*, vol. 162, pp. 1–5, 2012.

[16] X. Si, J. Zhang, F. Li et al., "Adjustable structure transition and improved gases (H_2, CO_2) adsorption property of metal-organic framework MIL-53 by encapsulation of BNHx," *Dalton Transactions*, vol. 41, no. 11, pp. 3119–3122, 2012.

[17] M. Anbia and S. Sheykhi, "Synthesis of nanoporous copper terephthalate [MIL-53 (Cu)] as a novel methane-storage adsorbent," *Journal of Natural Gas Chemistry*, vol. 21, no. 6, pp. 680–684, 2012.

[18] J. Jia, F. Xu, Z. Long, X. Hou, and M. J. Sepaniak, "Metal-organic framework MIL-53 (Fe) for highly selective and ultrasensitive direct sensing of $MeHg^+$," *Chemical Communications*, vol. 49, no. 41, pp. 4670–4672, 2013.

[19] W. Dong, X. Liu, W. Shi, and Y. Huang, "Metal-organic framework MIL-53 (Fe): facile microwave-assisted synthesis and use as a highly active peroxidase mimetic for glucose biosensing," *RSC Advances*, vol. 5, no. 23, pp. 17451–17457, 2015.

[20] G. Férey, M. Latroche, C. Serre, F. Millange, T. Loiseau, and A. Percheron-Guégan, "Hydrogen adsorption in the nanoporous metal-benzenedicarboxylate M (OH) $(O_2C - C_6H_4 - CO_2)$ $(M = Al_3^+, Cr_3^+)$, MIL-53," *Chemical Communications*, vol. 24, pp. 2976-2977, 2003.

[21] D. V. Patil, P. B. S. Rallapalli, G. P. Dangi, R. J. Tayade, R. S. Somani, and H. C. Bajaj, "MIL-53 (Al): an efficient adsorbent for the removal of nitrobenzene from aqueous solutions," *Industrial & Engineering Chemistry Research*, vol. 50, no. 18, pp. 10516–10524, 2011.

[22] M. Maes, F. Vermoortele, M. Boulhout et al., "Enthalpic effects in the adsorption of alkylaromatics on the metal-organic frameworks MIL-47 and MIL-53," *Microporous and Mesoporous Materials*, vol. 157, pp. 82–88, 2012.

[23] H.-P. Jing, C.-C. Wang, Y.-W. Zhang, P. Wang, and R. Li, "Photocatalytic degradation of methylene blue in ZIF-8," *RSC Advances*, vol. 4, no. 97, pp. 54454–54462, 2014.

[24] R. Liang, F. Jing, L. Shen, N. Qin, and L. Wu, "MIL-53 (Fe) as a highly efficient bifunctional photocatalyst for the simultaneous reduction of Cr (VI) and oxidation of dyes," *Journal of Hazardous Materials*, vol. 287, pp. 364–372, 2015.

[25] M. Pu, Y. Ma, J. Wan, Y. Wang, J. Wang, and M. L. Brusseau, "Activation performance and mechanism of a novel heterogeneous persulfate catalyst: metal-organic framework MIL-53 (Fe) with FeII/FeIII mixed-valence coordinatively unsaturated iron center," *Catalysis Science & Technology*, vol. 7, no. 5, pp. 1129–1140, 2017.

[26] E. Rahmani and M. Rahmani, "Al-based MIL-53 metal organic framework (MOF) as the new catalyst for friedel-crafts alkylation of benzene," *Industrial & Engineering Chemistry Research*, vol. 57, no. 1, pp. 169–178, 2018.

[27] M. T. Thanh, T. V. Thien, P. D. Du, N. P. Hung, and D. Q. Khieu, "Iron doped zeolitic imidazolate framework (Fe-ZIF-8): synthesis and photocatalytic degradation of RDB dye in Fe-ZIF-8," *Journal of Porous Materials*, vol. 25, no. 3, pp. 857–869, 2018.

[28] T. Devic, P. Horcajada, C. Serre et al., "Functionalization in flexible porous solids: effects on the pore opening and the host–guest interactions," *Journal of the American Chemical Society*, vol. 132, no. 3, pp. 1127–1136, 2010.

[29] L. Chen, J. P. S. Mowat, D. Fairen-Jimenez et al., "Elucidating the breathing of the metal-organic framework MIL-53 (Sc) with ab initio molecular dynamics simulations and in situ X-ray powder diffraction experiments," *Journal of the American Chemical Society*, vol. 135, no. 42, pp. 15763–15773, 2013.

[30] D. T. C. Nguyen, H. T. N. Le, T. S. Do et al., "Metal-Organic Framework MIL-53 (Fe) as an adsorbent for ibuprofen drug removal from aqueous solutions: response surface modeling and optimization," *Journal of Chemistry*, vol. 2019, Article ID 5602957, 2019.

[31] A. D. Bokare and W. Choi, "Review of iron-free Fenton-like systems for activating H_2O_2 in advanced oxidation processes," *Journal of Hazardous Materials*, vol. 275, pp. 121–135, 2014.

[32] F. Martínez, G. Calleja, J. A. Melero, and R. Molina, "Heterogeneous photo-Fenton degradation of phenolic aqueous solutions over iron-containing SBA-15 catalyst," *Applied Catalysis B: Environmental*, vol. 60, no. 3-4, pp. 181–190, 2005.

[33] Y. Huang, C. Cui, D. Zhang, L. Li, and D. Pan, "Heterogeneous catalytic ozonation of dibutyl phthalate in aqueous solution in the presence of iron-loaded activated carbon," *Chemosphere*, vol. 119, pp. 295–301, 2015.

[34] S. Guo, G. Zhang, and J. Wang, "Photo-Fenton degradation of rhodamine B using Fe_2O_3-Kaolin as heterogeneous catalyst: characterization, process optimization and mechanism," *Journal of Colloid and Interface Science*, vol. 433, pp. 1–8, 2014.

[35] D. Q. Khieu, D. T. Quang, T. D. Lam, N. H. Phu, J. H. Lee, and J. S. Kim, "Fe-MCM-41 with highly ordered mesoporous structure and high Fe content: synthesis and application in heterogeneous catalytic wet oxidation of phenol," *Journal of Inclusion Phenomena and Macrocyclic Chemistry*, vol. 65, no. 1-2, pp. 73–81, 2009.

[36] P. D. Du, H. T. Danh, P. N. Hoai, N. M. Thanh, V. T. Nguyen, and D. Q. Khieu, "Heterogeneous UV/Fenton-like degradation of methyl orange using iron terephthalate MIL-53 catalyst," *Journal of Chemistry*, vol. 2020, Article ID 1474357, 2020.

[37] G. Bharath, S. Anwer, R. V. Mangalaraja, E. Alhseinat, F. Banat, and N. Ponpandian, "Sunlight-induced photochemical synthesis of Au nanodots on α-Fe_2O_3 @ reduced graphene oxide nanocomposite and their enhanced heterogeneous catalytic properties," *Scientific Reports*, vol. 8, no. 1, p. 5718, 2018.

[38] S. Ramazanov, D. Sobola, F. Orudzhev et al., "Surface modification and enhancement of ferromagnetism in $BiFeO_3$ nanofilms deposited on HOPG," *Nanomaterials*, vol. 10, no. 10, p. 1990, 2020.

[39] Q. Wang, S. Tian, J. Long, and P. Ning, "Use of Fe (II) Fe (III)-LDHs prepared by co-precipitation method in a heterogeneous-Fenton process for degradation of methylene blue," *Catalysis Today*, vol. 224, pp. 41–48, 2014.